

Magnetic Bistability and Single-Crystal-to-Single-Crystal Transformation Induced by Guest Desorption

Masayuki Nihei, Lingqin Han, and Hiroki Oshio*

Graduate School of Pure and Applied Sciences, University of Tsukuba, Tennodai 1-1-1, Tsukuba, Ibaraki, Japan

Received December 20, 2006; E-mail: oshio@chem.tsukuba.ac.jp

Porous compounds have attracted much interest from view points of gas separation,¹ gas storage,² selective guest sorption,³ and sensors.⁴ Recently, metal–organic open frameworks (MOFs), coordination polymers with infinite structures, have shown intriguing physical properties such as solvent-induced ferri/ferromagnetism.⁵ Especially, molecular systems, which show single-crystal-to-single-crystal transformations that are associated with physical property changes, are very important for applications in sensors;⁶ however, the number of such molecular systems is still limited.⁷ Iron(II) complexes with tridentate 2,6-di(pyrazol-1-yl)pyridine (dpp) ligands and their derivatives show thermally induced spin-crossover (SC) between high-spin (HS) and low-spin (LS) states.⁸ Introduction of bulky groups to SC complexes may make large space in the crystals, such as MOFs, which accommodate lattice solvent molecules, and thus, there may be synergistic behavior due to magnetism and solvent adsorption. We prepared a new tridentate ligand with a bulky ferrocenyl group, and magnetic properties of its iron(II) complex, $[\text{Fe}(\text{dppFc})_2](\text{BF}_4)_2 \cdot 2\text{Et}_2\text{O}$ ($\mathbf{1} \cdot 2\text{Et}_2\text{O}$, $\text{dppFc} = 1\text{-ferrocenyl-2-}\{(2,6\text{-bis(pyrazolyl)pyridyl)ethylene}\}$), were studied. Complex $\mathbf{1} \cdot 2\text{Et}_2\text{O}$ showed single-crystal-to-single-crystal transformation associated with release of crystal solvent molecules, and its SC behavior was perturbed by release of solvent molecules.

The tridentate ligand dppFc was synthesized starting from 2,6-di(pyrazol-1-yl)-4-hydroxymethylpyridine.⁸ Reaction of dppFc with $\text{Fe}(\text{BF}_4)_2 \cdot 6\text{H}_2\text{O}$ in methanol, followed by recrystallization from nitromethane/diethyl ether, yielded purple lozenge crystals of $\mathbf{1} \cdot 2\text{Et}_2\text{O}$ in the yield of 38%. X-ray crystal structure analysis for $\mathbf{1} \cdot 2\text{Et}_2\text{O}$ was performed at 110 K,⁹ and an ORTEP diagram of the complex cation is depicted in Figure 1. Complex $\mathbf{1} \cdot 2\text{Et}_2\text{O}$ crystallized in the orthorhombic space group $Fdd2$, and the asymmetric unit contained half of the complex cation, one anion and one diethyl ether molecule. The central iron(II) ion was coordinated by six nitrogen atoms from two tridentate dppFc , giving distorted octahedral coordination geometry. Coordination bond lengths of $\text{Fe}-\text{N1}$ (pyridyl), $\text{Fe}-\text{N2}$ (pyrazolyl), and $\text{Fe}-\text{N4}$ (pyrazolyl) were 2.086(3), 2.161(3), and 2.185(3) Å, respectively, which are characteristic of typical HS iron(II) ions. Distortion of the coordination geometry from the ideal octahedron was quantified using Σ parameters ($=\sum|(90 - q)|$ (°), q = bite angles of the two coordinated ligands). Larger Σ values, which signify larger distortions from the ideal octahedral coordination sphere, correspond to a weaker ligand field strength on an iron(II) ion.¹⁰ The Σ value for the central iron(II) ion in $\mathbf{1} \cdot 2\text{Et}_2\text{O}$ was 144.7°, which suggests that the iron(II) ion is in the HS state.⁸ Figure 2(top) shows a crystal packing diagram of $\mathbf{1} \cdot 2\text{Et}_2\text{O}$. In $\mathbf{1} \cdot 2\text{Et}_2\text{O}$, the complex cations form a 3D network by interacting with each other via BF_4^- , where interatomic distances of the dpp hydrogen atoms with fluorine atoms of BF_4^- were in the range of 2.362–2.687 Å. Diethyl ether molecules are located in the voids constructed by the complex cations and anions.

The single crystal of $\mathbf{1} \cdot 2\text{Et}_2\text{O}$, the same crystal used for the X-ray structure analysis, was allowed to stand for a week, and $\mathbf{1} \cdot 2\text{Et}_2\text{O}$

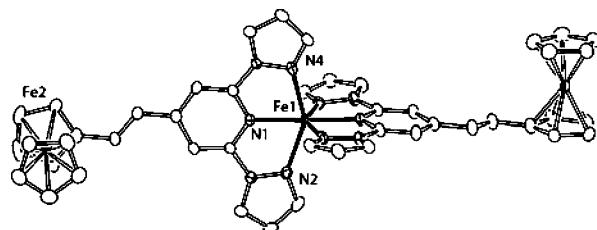


Figure 1. An ORTEP diagram of the cation molecule in $\mathbf{1} \cdot 2\text{Et}_2\text{O}$.

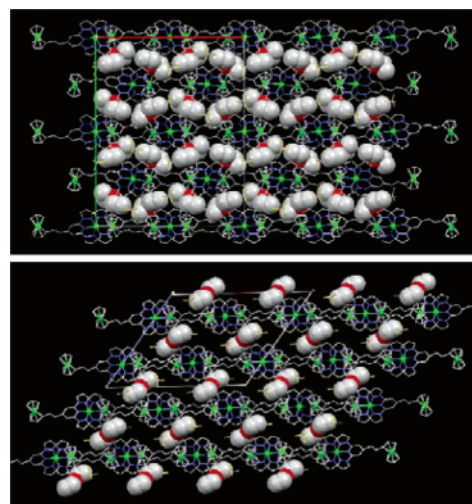


Figure 2. Crystal packing of $\mathbf{1} \cdot 2\text{Et}_2\text{O}$ (top) and $\mathbf{1} \cdot \text{Et}_2\text{O}$ (bottom).

lost one Et_2O molecule to yield $\mathbf{1} \cdot \text{Et}_2\text{O}$ ⁹ (Figure 2, bottom). No significant loss of crystallinity was observed during the release of the solvent molecules, which might be due to the stable 3D networks. Thermogravimetric measurements for $\mathbf{1} \cdot 2\text{Et}_2\text{O}$ showed a two-step weight loss at 50 and 120 °C, of which each step corresponds to the release of diethyl ether molecules (Figure S1). X-ray structure determinations of $\mathbf{1} \cdot \text{Et}_2\text{O}$ at 110 and 300 K showed that the crystal system was the monoclinic space group $C2/c$,⁹ and the complex molecule was located on a 2-fold axis. Coordination geometry about the central iron(II) ion in $\mathbf{1} \cdot \text{Et}_2\text{O}$ at 110 K was different from that in $\mathbf{1} \cdot 2\text{Et}_2\text{O}$. The average coordination bond length and Σ value were 1.952 Å and 90.5°, respectively, which are characteristic of LS iron(II) ions. Upon increasing the temperature to 300 K, the crystal system of $\mathbf{1} \cdot \text{Et}_2\text{O}$ did not change, but obvious structural changes on the iron(II) center were observed. The average coordination bond length and Σ value for $\mathbf{1} \cdot \text{Et}_2\text{O}$ were 2.095 Å and 138.0°, respectively, at 300 K, and these changes suggest that iron(II) ion converts to HS at higher temperature. When the single crystal of $\mathbf{1} \cdot \text{Et}_2\text{O}$ was exposed to diethyl ether, it adsorbed one Et_2O molecule to be $\mathbf{1} \cdot 2\text{Et}_2\text{O}$, of which crystallographic parameters were identical to those for the initial $\mathbf{1} \cdot 2\text{Et}_2\text{O}$.⁹

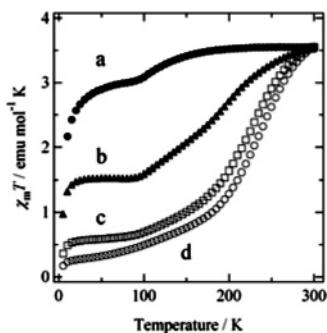


Figure 3. $\chi_m T$ - T plots for $1 \cdot 2\text{Et}_2\text{O}$ after storage for (a) 0 min, (b) 10 min, (c) 1 h, and (d) 4 h.

Magnetic susceptibility measurements for $1 \cdot 2\text{Et}_2\text{O}$ were performed down to 1.8 K, and susceptibility changes upon losing solvent molecules were investigated for the same sample in the SQUID magnetometer (Figure 3).¹¹ The $\chi_m T$ values of $1 \cdot 2\text{Et}_2\text{O}$ were nearly constant (3.52 $\text{emu mol}^{-1} \text{K}$, at 300 K) down to 150 K, suggesting a HS iron(II) ion. A sudden decrease in the $\chi_m T$ values below 30 K is due to magnetic anisotropy of the HS iron(II) ion. Anomaly observed around 100 K is due to the structural changes occurring in the central HS iron(II) ion, which was confirmed by Mössbauer spectra (Figure S2).¹² Upon losing one solvent molecule from $1 \cdot 2\text{Et}_2\text{O}$, the $\chi_m T$ values showed a different temperature profile from the original $1 \cdot 2\text{Et}_2\text{O}$, and after storing the sample at 300 K for 4 h in the SQUID magnetometer, the $\chi_m T$ - T curve became identical to that for $1 \cdot \text{Et}_2\text{O}$.

The $\chi_m T$ value for $1 \cdot \text{Et}_2\text{O}$ is 3.55 $\text{emu mol}^{-1} \text{K}$ at 300 K, which corresponds to the Curie constant for a HS iron(II) ion. As the temperature was lowered, the $\chi_m T$ value decreased gradually and reached a value of 0.26 $\text{emu mol}^{-1} \text{K}$ at 20 K. The temperature dependence of the $\chi_m T$ values confirmed the occurrence of a thermal spin transition to the LS state with $T_c = 230 \text{K}$, which is in good agreement with the X-ray crystallographic analyses. The nonzero $\chi_m T$ values at lower temperature might be due to the small amount of paramagnetic impurity. It should be noted that re-solvation was achieved by exposing the sample to diethyl ether and that the $\chi_m T$ - T curve for the initial $1 \cdot 2\text{Et}_2\text{O}$ was fully recovered (Figure S3). It is also pointed out that the magnetic property of the non-solvated **1**, prepared by storing $1 \cdot \text{Et}_2\text{O}$ at 400 K for 6 h in the SQUID magnetometer, is similar to that of $1 \cdot 2\text{Et}_2\text{O}$.¹³

The iron(II) ion in $1 \cdot 2\text{Et}_2\text{O}$ was in a HS state over the entire temperature range measured, and upon losing one solvent molecule, the complex showed SC behavior. Solvent molecules in the crystal affects the SC behavior, and it has often been observed that the loss of protic solvent molecules destabilizes the LS state.¹⁴ The complex cation in $1 \cdot \text{Et}_2\text{O}$ had no intermolecular interaction with the diethyl ether molecules, while $1 \cdot 2\text{Et}_2\text{O}$ had C-H $\cdots\pi$ and C-H $\cdots\text{O}$ interactions between the complex and aprotic diethyl ether molecules (Figure S4). It is noted that $1 \cdot 2\text{Et}_2\text{O}$ has more organized supramolecular structure, and this may affect spin-crossover behaviors.¹⁵ In addition, the close intermolecular contacts stress the coordination environment around the HS iron(II) ion, which is reflected in the different Σ values (144.7 and 137.97° for $1 \cdot 2\text{Et}_2\text{O}$ and $1 \cdot \text{Et}_2\text{O}$, respectively). The smaller Σ value implies a stronger ligand field leading to the stabilization of LS state, and $1 \cdot \text{Et}_2\text{O}$ exhibited SC behavior.

In summary, an iron(II) complex of $1 \cdot 2\text{Et}_2\text{O}$ was prepared, and the presence of a unique single-crystal-to-single-crystal transformation with significant magnetic property changes was confirmed by X-ray crystallographic analysis and magnetic measurements. Complex $1 \cdot 2\text{Et}_2\text{O}$ has redox-active ferrocenyl groups; therefore, the system should be active toward specific redox reactions in nanosized space. Studies to introduce redox-active molecules into the space are currently in progress.

Acknowledgment. This work was partially supported by a Grant-in-Aid for Scientific Research from the Ministry of Education, Culture, Sports, Science and Technology, Japan.

Supporting Information Available: Experimental details, additional figures, and X-ray crystallographic files in CIF format. This material is available free of charge via the Internet at <http://pubs.acs.org>.

References

- (1) Kuznicki, S. M.; Bell, V. A.; Nair, S.; Hillhouse, H. W.; Jacobinas, R. M.; Braunbarth, C. M.; Toby, B. H.; Tspatsis, M. *Nature* **2001**, *412*, 720.
- (2) (a) Matsuda, R.; Kitaura, R.; Kitagawa, S.; Kubota, Y.; Belosludov, R. V.; Kobayashi, T. C.; Sakamoto, H.; Chiba, T.; Takata, M.; Kawazoe, Y.; Mita, Y. *Nature* **2005**, *436*, 238. (b) Kitaura, R.; Kitagawa, S.; Kubota, Y.; Kobayashi, T.; Kindo, L.; Mita, Y.; Matsuo, A.; Kobayashi, M.; Chang, H.-C.; Ozawa, T.; Suzuki, M.; Sakata, M.; Takata, M. *Science* **2002**, *298*, 2358.
- (3) (a) Chae, H. K.; Siberio-Perez, D. Y.; Kim, J. H.; Go, Y. B.; Yaghi, O. M. *Nature* **2004**, *427*, 523. (b) Yaghi, O. M.; Li, G. M.; Li, H. L. *Nature* **1995**, *378*, 703.
- (4) Albrecht, M.; Lutz, M.; Spek, A. L.; van Koten, G. *Nature* **2000**, *406*, 970.
- (5) (a) Maspoeh, D.; Ruiz-Molina, D.; Wurst, K.; Domingo, N.; Cavallini, M.; Biscarini, F.; Tejada, J.; Rovira, C.; Veciana, J. *Nat. Mater.* **2003**, *2*, 190. (b) Yanai, N.; Kaneko, W.; Yoneda, K.; Ohba, M.; Kitagawa, S. *J. Am. Chem. Soc.* **2007**, *129*, 3496.
- (6) (a) Suh, M. P.; Moon, H. R.; Lee, E. Y.; Jang, S. Y. *J. Am. Chem. Soc.* **2006**, *128*, 4710. (b) Choi, H. J.; Suh, M. P. *J. Am. Chem. Soc.* **2004**, *126*, 15844. (c) Zhang, J.-P.; Lin, Y.-Y.; Zhang, W.-X.; Chen, X.-M. *J. Am. Chem. Soc.* **2005**, *127*, 14162.
- (7) (a) Halder, G. J.; Kepert, C. J. *Aust. J. Chem.* **2006**, *59*, 597. (b) Amoree, J. J. M.; Kepert, C. J.; Cashion, J. D.; Moubaraki, B.; Neville, S. M.; Murray, K. S. *Chem.-Eur. J.* **2006**, *12*, 8220.
- (8) (a) Carbonera, C.; Costa, J. S.; Money, V. A.; Elhaik, J.; Howard, A. K.; Halcrow, M. A.; Létard, J.-F. *J. Chem. Soc., Dalton Trans.* **2006**, 3058. (b) Money, V. A.; Elhaik, J.; Halcrow, M. A.; Howard, J. A. K. *J. Chem. Soc., Dalton Trans.* **2004**, 1516.
- (9) Crystal data for $1 \cdot 2\text{Et}_2\text{O}$ at 110 K: $\text{C}_{54}\text{H}_{58}\text{N}_{10}\text{B}_2\text{F}_8\text{Fe}_3\text{O}_2$, orthorhombic *Fdd2*, $a = 25.544(2) \text{Å}$, $b = 32.347(4) \text{Å}$, $c = 12.809(2) \text{Å}$, $V = 10584.1(10) \text{Å}^3$, $Z = 8$, $d_{\text{calcd}} = 1.532 \text{g cm}^{-3}$, 18 574 reflections measured, 6510 unique reflections ($R_{\text{int}} = 0.0273$). Final $R1 = 0.0526$ and $wR2 = 0.1354$ ($I > 2\sigma I$). Crystal data for $1 \cdot \text{Et}_2\text{O}$ at 110 K: $\text{C}_{50}\text{H}_{48}\text{N}_{10}\text{B}_2\text{F}_8\text{Fe}_3\text{O}_2$, monoclinic *C2/c*, $a = 25.04(2) \text{Å}$, $b = 12.792(12) \text{Å}$, $c = 19.806(19) \text{Å}$, $V = 5108(8) \text{Å}^3$, $Z = 4$, $d_{\text{calcd}} = 1.490 \text{g cm}^{-3}$, 14 068 reflections measured, 5520 unique reflections ($R_{\text{int}} = 0.0558$). Final $R1 = 0.1290$ and $wR2 = 0.3306$ ($I > 2\sigma I$); at 300 K: monoclinic *C2/c*, $a = 25.42(2) \text{Å}$, $b = 12.686(12) \text{Å}$, $c = 20.653(19) \text{Å}$, $V = 5350(8) \text{Å}^3$, $Z = 4$, $d_{\text{calcd}} = 1.423 \text{g cm}^{-3}$, 15 348 reflections measured, 5886 unique reflections ($R_{\text{int}} = 0.0481$). Final $R1 = 0.1135$ and $wR2 = 0.3457$ ($I > 2\sigma I$). Crystal data for re-solvated $1 \cdot 2\text{Et}_2\text{O}$ at 200 K: $\text{C}_{54}\text{H}_{58}\text{N}_{10}\text{B}_2\text{F}_8\text{Fe}_3\text{O}_2$, orthorhombic, $a = 25.469(9) \text{Å}$, $b = 33.352(1) \text{Å}$, $c = 12.855(5) \text{Å}$, $V = 10919.6(12) \text{Å}^3$.
- (10) Guionneau, P.; Marchivie, M.; Bravic, G.; Létard, J.-F.; Chasseau, D. *J. Mater. Chem.* **2002**, *12*, 2546.
- (11) The sample was kept in the SQUID magnetometer at 300 K for the periods described in the figure caption to remove solvent molecules.
- (12) Mössbauer spectroscopic measurements of $1 \cdot 2\text{Et}_2\text{O}$ showed substantial changes in the Mössbauer parameters for the HS iron(II) species from ($\delta = 1.09 \text{mm/s}$, $\Delta = 1.53 \text{mm/s}$) at 130 K to ($\delta = 0.97 \text{mm/s}$, $\Delta = 1.84 \text{mm/s}$) at 20 K, which was due to the changes in coordination environments of the iron(II) centers.
- (13) **1** is not a single crystal and is readily hydrated by air moisture.
- (14) (a) Gütllich, P.; Goordwin, H. A. *Chem. Soc. Rev.* **2000**, *29*, 419. (b) Halder, G. J.; Kepert, C. J.; Moubaraki, B.; Murray, K. S.; Cashion, J. D. *Science* **2002**, *298*, 1762. (c) Leita, B. A.; Moubaraki, B.; Murray, K. S.; Smith, J. P. *Polyhedron* **2005**, *24*, 2165.
- (15) Reger, D. L.; Gardinier, J. R.; Smith, M. D.; Shahin, A. M.; Long, G. J.; Rebbouh, L.; Grandjean, F. *Inorg. Chem.* **2005**, *44*, 1852.

JA069120I